Time-Resolved Small-Angle X-ray Scattering Studies of Spinodal Decomposition Kinetics in a Semidilute Polystyrene−Dioctyl Phthalate Solution

Yonglin Xie,*,†,‡ Karl F. Ludwig, Jr.,† Rama Bansil,†,§ Patrick D. Gallagher,†,§,⊥ Čestmír Koňák,‖ and Guarionex Morales†

Department of Physics and Center for Polymer Studies, Boston University, Boston, Massachusetts 02215, and Institute of Macromolecular Chemistry, Academy of Sciences of the Czech Republic, Czech Republic

Received February 8, 1995; Revised Manuscript Received February 27, 1996[⊗]

ABSTRACT: Synchrotron-based time-resolved small-angle X-ray scattering was used to measure the early-stage spinodal decomposition kinetics in a highly viscous semidilute solution of polystyrene in dioctyl phthalate. Although strong nonlinearities in the kinetics were observed, a linear theory analysis could fit the evolution of the structure factor at short times and low wavenumbers. Nonlinearities become significant earlier at higher wavenumbers, which is consistent with recent computer simulation studies. From the linear theory analysis, the exponential relaxation rate of the structure factor $R(q)$ was found to be linear in q^2 in the low-wavenumber region of the experiments, in agreement with mean-field theory for spinodal decomposition in polymer solutions. The wavenumber-dependent Onsager transport coefficient $\Lambda(q)$, which is the Fourier transform of the nonlocal mobility in a polymer system, was determined to scale as q^{-4}. This q dependence, which is stronger than that predicted by existing theory, may be related to entanglement effects.

1. Introduction

When a binary system is quenched from its one-phase equilibrium state outside the coexistence curve into the two-phase region beyond the spinodal line, it becomes unstable and phase separates via a spinodal decomposition process. Despite several decades of extensive experimental and theoretical studies,[1] our understanding of the kinetics of spinodal decomposition is still limited.

Conventionally, the process of spinodal decomposition is conceptually divided into three time regions: early, intermediate, and late stages. In the early stage, the growth of concentration fluctuations is small compared to the average concentration, so that coupling between fluctuations can often be neglected. In the intermediate stage, the amplitude of concentration fluctuations continues increasing toward the equilibrium concentrations while well-defined domains form, grow in size, and sharpen their domain walls. In the late stage, domains with equilibrium concentration coarsen. The late-stage process obeys dynamic scaling laws.

The kinetics of early-stage spinodal decomposition in polymer blends has been widely studied.[2] Experimental results have most often been compared with linear theory, which was originally formulated to describe the early-stage spinodal decomposition process in metallic alloys[3,4] and modified later by de Gennes,[5] Pincus,[6] and Binder[7] to apply to polymer systems. Generally good agreement between theory and experiment has been reported. Yet there are few studies of kinetics in polymer solutions. A major reason for this is that early-stage kinetics in solutions is often too fast to be recorded, especially at high wavenumbers where the kinetics is faster than at low wavenumbers. Only recently have there been light scattering studies of the kinetics of spinodal decomposition in polymer solutions.[8,9] Linear theory was found to be valid for the early stage of the spinodal decomposition process in these reports. Late-stage scaling behavior was also observed. Since the wavenumber range accessible to light scattering is approximately 5×10^{-5} Å $< q < 3 \times 10^{-3}$ Å, light scattering can only provide structural information on length scales larger than approximately 500 Å. Small-angle X-ray scattering (SAXS) and small-angle neutron scattering (SANS) are complementary to light scattering because their wavenumber range (5×10^{-3} Å $< q < 5 \times 10^{-1}$ Å) covers the characteristic size of individual polymers R_g as well as the correlation length ξ of concentration fluctuations for quenches more than a few degrees below the spinodal line. Nevertheless, to our knowledge, no SAXS or SANS studies of spinodal decomposition kinetics in polymer solutions have been reported thus far.

In this paper, we report a time-resolved SAXS study of the spinodal decomposition kinetics of a semidilute polymer solution of polystyrene (PS) in the viscous Θ-solvent dioctyl phthalate (DOP). The use of this viscous Θ-solvent ($\eta \approx 300$ cps at 0 °C) at semidilute PS concentration allowed us to slow down the spinodal decomposition kinetics significantly. This combined with the high flux of synchrotron radiation enabled us to study the early-stage spinodal decomposition kinetics in the solution. A good statistical counting rate was obtained at relatively short time scales (1 s), despite the weak scattering from the solutions. Nonlinearities in the kinetics were observed to occur first at high wavenumbers. A similar phenomenon has been observed in a computer simulation study of spinodal decomposition kinetics in Ising models[10] and X-ray scattering studies of spinodal decomposition kinetics in Al−Zn alloys.[11] We know of no theory which adequately describes the kinetics of spinodal decomposition in polymer solutions over the entire time scale examined. However, a linear analysis could fit the evolution of the structure factor

† Department of Physics, Boston University.
‡ Current address: Joseph C. Wilson Center for Technology, Xerox Corp., Webster, NY 14580.
§ Center for Polymer Studies, Boston University.
⊥ Current address: National Institute of Standards and Technology, Gaithersburg, MD 20899.
‖ Academy of Sciences of the Czech Republic.
⊗ Abstract published in *Advance ACS Abstracts,* August 15, 1996.

S0024-9297(95)00153-7 CCC: $12.00

during the phase separation process at early times and low wavenumbers. We were able to extract both the exponential relaxation rate (amplification factor) $R(q)$ of the structure factor and the wavenumber-dependent Onsager coefficient $\Lambda(q)$, which is the Fourier transform of the nonlocal mobility characteristic of a polymer system.[5−7] These quantities describe the early-stage kinetics of the phase separation process. Moreover, as Binder[7] has pointed out, a linear theory analysis also yields fundamental information about polymer solution dynamics on length scales comparable to R_g, which is not easily obtained with other approaches. Since it is essentially a linear response formulation, experimental quantities derived using linear theory should also describe the equilibrium dynamics of the solution.

2. Theoretical Background

According to the mean-field theory of a polymer in a Θ-solvent at equilibrium in the one-phase region, the structure factor of concentration fluctuations at low wavenumbers is given by the Ornstein−Zernicke Lorentzian function[12,13]

$$S_L(q) = \frac{S_L(0)}{1 + \xi^2 q^2} \quad \text{for} \quad q\xi \ll 1 \tag{1}$$

Here $S_L(0)$ is the extrapolated structure factor at zero angle and ξ is the correlation length of the concentration fluctuations. Theory predicts power law behavior for $S_L(0)$ and ξ as the critical point or spinodal point is approached, i.e.,

$$\xi = \xi_0 \epsilon^{-\nu} \quad \text{and} \quad S_L(0) = S_0 \epsilon^{-\gamma} \tag{2}$$

where ξ_0 and S_0 are constants and ϵ is the reduced temperature, $\epsilon = T/T_s - 1$. The prefactor ξ_0 is a length scale comparable to the effective range of interaction in the system.

Deviations from the Ornstein−Zernicke function have been repeatedly reported in equilibrium studies of semidilute polymer solutions. A number of experiments[14−18] revealed an "excess scattering" at low wavenumbers in semidilute polymer solutions which indicates enhanced concentration fluctuations in these systems. Although many attempts have been made to account for this effect, no conclusive explanation has been reached. Koberstein *et al.*[16] have suggested that the "excess scattering" is caused by long-range random heterogeneities, with correlation lengths several times the radius of gyration of the dissolved polymer. They found that the Debye−Bueche theory for a random heterogeneous system[19] provided satisfactory fits to their data. According to Koberstein *et al.*, the total structure factor can be expressed as

$$S(q) = S_L(q) + S_{ex}(q) \tag{3}$$

where the normal component $S_L(q)$ has the Ornstein−Zernicke Lorentzian form as in eq 1, and the "excess scattering" component $S_{ex}(q)$ takes the from

$$S_{ex}(q) = \frac{8\pi\bar{\eta}^2\zeta^3/n}{(1 + \zeta^2 q^2)^2} \tag{4}$$

Here n is the number density of monomers, $\bar{\eta}^2$ is the mean square fluctuation in concentration, and ζ is an average correlation length of random heterogeneities.

If nonlinear terms coupling fluctuations of different wavenumber are neglected, a linearized equation of motion for the structure factor $S(q,t)$ in a polymer system undergoing spinodal decomposition can be written:

$$\frac{\partial S(q,t)}{\partial t} = 2R(q)S(q,t) + 2k_B T\Lambda(q)q^2 \tag{5}$$

If the static solution of eq 5 is denoted $S(q,\infty)$, then

$$R(q) = -k_B T\Lambda(q)q^2 S^{-1}(q,\infty) \tag{6}$$

For a quench within the one-phase region, $S(q,\infty)$ is the equilibrium structure factor at the quench temperature. For a quench into the spinodal region, $S(q,\infty)$ is a virtual structure factor which is the extrapolated final collective structure factor at the quench temperature according to the linear theory. The virtual structure factor is never reached physically.

The solution of eq 5 can be written as

$$S(q,t) = S(q,\infty) + [S(q,0) - S(q,\infty)]e^{2R(q)t} \tag{7}$$

Here $S(q,0)$ is the initial structure factor when the temperature reaches equilibrium after a quench into the unstable two-phase region. Thus, according to linear theory, the structure factor is a monotonic function of time and undergoes an exponential growth for $R(q) > 0$ and an exponential relaxation for $R(q) < 0$. This is a direct result of the linear approximation.

We know of no kinetics theory which properly treats $R(q)$, $S(q,\infty)$, or $\Lambda(q)$ in the semidilute concentration regime in which this study was performed. However, Binder[7] has developed a linear theory analysis of spinodal decomposition in polymer blends which he was able to apply in a very approximate manner to solutions. In Binder's approach the virtual structure factor is calculated using a random-phase approximation (RPA):[20]

$$S(q,\infty)^{-1} = [\phi S_A(q)]^{-1} + v_2 + v_3\phi \tag{8}$$

where v_2 and v_3 are the second and third virial coefficients at the quench temperature, ϕ is the volume fraction, and $S_A(q)$ is the single-chain structure factor which, in the noninteracting case, is the Debye function $f_D(x)$:

$$S_A(q) = Nf_D(x) = N\frac{2}{x}\left[1 - \frac{1 - e^{-x}}{x}\right] \tag{9}$$

Here N is the degree of polymerization of a polymer chain and $x = R_g^2 q^2$ with R_g being the radius of gyration of a polymer chain. It is important to note that in the equilibrium one-phase region of the polymer−solution phase diagram, this approach does not reproduce the proper screening effects in semidilute solutions[12] nor does it exhibit the widely observed "excess scattering". Thus its extension into the spinodal region is also questionable in semidilute concentrations. Below the spinodal, the RPA $S(q,\infty)$ diverges and changes sign from negative to positive at a critical wavenumber q_c given by the condition that the right-hand-side of eq 8 vanishes. Typically, the critical wavenumber is comparable to (or sometimes defined as) the inverse correlation length ξ^{-1}. The second virial coefficient v_2 decreases with decreasing temperature (increasing quench depth) in PS−DOP so the value of q_c increases

with increasing quench depth. Since eq 6 shows that the amplification factor $R(q)$ is inversely proportional to $-S(q,\infty)$, this implies that $R(q)$ changes sign from positive to negative at q_c, i.e. that the evolution of the structure factor changes from exponential growth to exponential relaxation.

In Binder's theory, the Onsager coefficient is proportional to the single-chain structure factor of an ideal polymer chain:

$$\Lambda(q) \propto S_A(q) \tag{10}$$

At low wavenumbers, $qR_g < 1$, this suggests that $\Lambda(q)$ scales as $(1 - q^2 R_g^2/3)$. Previous light scattering studies of spinodal decomposition kinetics in solutions[8,21] could not detect the wavenumber dependence of $\Lambda(q)$ because the mobility is constant in the light scattering wavenumber region. Even in the case of polymer blends, which have been widely studied with SAXS and SANS, there have been few studies measuring the wavenumber dependence of the Onsager mobility.[22,23] Generally, their results have been qualitatively consistent with Binder's calculation. As discussed below, however, we have found very different behavior for $\Lambda(q)$ in semidilute solution.

3. Experimental Techniques

The experiments reported here were performed at the X-20C beamline of the National Synchrotron Light Source at Brookhaven National Laboratory and used a high flux multilayer monochromator and a position sensitive detector.[24] The photon energy used was 7.0 keV, which corresponds to a wavelength $\lambda = 1.8$ Å. The detector was positioned approximately 95 cm away from the sample to obtain a wavenumber range of 0.004 Å^{-1} < q < 0.075 Å^{-1}. The absolute incident beam intensity was monitored with a helium-filled ion chamber and also independently determined by measuring the attenuated direct beam on the diode array detector.

Samples were sealed between two thin flat kapton windows, which themselves contributed very little X-ray scattering. The sample thicknesses were approximately 2 mm. The linear polystyrene polymer used was purchased from Polysciences Inc. with molecular weight $M_w = 90\,000$ and polydispersity $M_n/M_w = 1.04$. The polymer was first dissolved in tetrahydrofuran and filtered to remove any dust impurities. Then the dried polymer was dissolved in DOP and maintained at an elevated temperature of $T = 50$ °C for 72 h. The solutions were degased before filling.

The Θ-temperature for the PS−DOP solution is reported to be Θ = 22.0 °C.[25] The radius of gyration for polystyrene of molecular weight $M_w = 90\,000$ in dioctyl phthalate is estimated to be $R_g(\Theta) \approx 100$ Å. The overlap concentration c^* at the Θ-temperature can be calculated using the relation given by des Cloizeaux,[26] $c^* \sim 0.053$ g·cm^{-3}. The concentration of the solution studied was $c = 0.26$ g·cm$^{-3} \approx 5c^*$. It is difficult to determine exactly the critical concentration c_c for PS−DOP solutions due to the lack of experimental data. The cloud point of the sample studied was determined to be approximately −10 °C by light transmission experiments through temperature cycles. Two independent SAXS experiments were performed 6 months apart using different slit sizes on the same sample; they both lead to the same conclusions. The long time reproducibility of the measurements indicates that there is no observable radiation damage to the sample by the X-ray beam.

4. Data Analysis and Results

The empty kapton cell scattering was carefully subtracted from the total scattering, and the scattering patterns were normalized to an absolute scale per monomer using the ion chamber current to correct for any change of the incident beam intensity or sample absorption. The relative accuracy of the normalization is better than 10%, although the absolute accuracy is more difficult to assess. Data were deconvolved to account for the smearing effect of the finite pixel size of the detector and the finite beam spot size. Details of the normalization and deconvolution process will be discussed in another paper.[18]

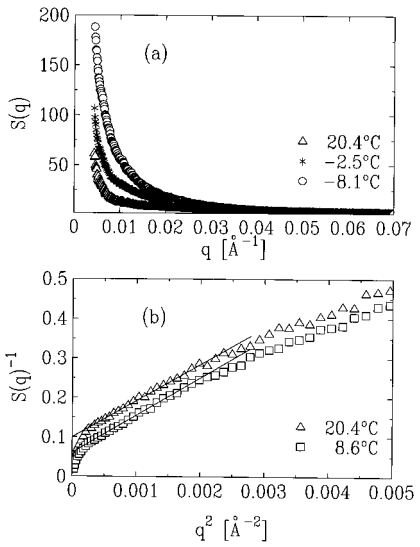

Figure 1. (a) Equilibrium structure factor at three different temperatures. (b) Zimm representation of equilibrium structure factors at two different temperatures. Lines are linear fits to the intermediate wavenumber range 0.02 Å < q < 0.04 Å.

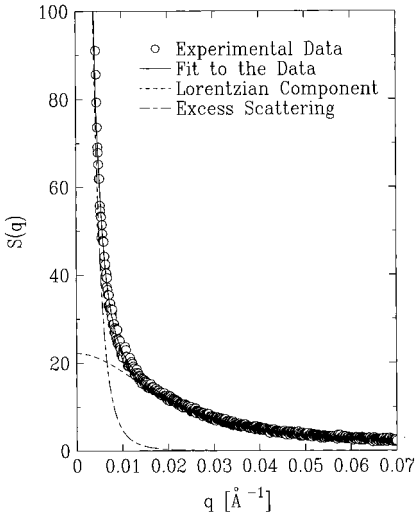

Figure 2. Fit of the equilibrium structure factor at $T = 3.1$ °C to eq 3.

4.1. Equilibrium Measurements. The absolute equilibrium structure factors at temperatures ranging from +20.5 down to −8.1 °C in the equilibrium single-phase region are presented in Figure 1a. As the spinodal point is approached, a divergence of the concentration fluctuations occurs; this is observed in the X-ray scattering experiment as an enhancement of the small-angle scattering.

The function in eq 3 has been fit to our measured equilibrium structure factors using a nonlinear fit method. A typical fit is shown in Figure 2. The temperature dependence of the parameters for the Lorentzian component is plotted in Figure 3, and those of the "excess scattering" are plotted in Figure 4. As the spinodal point is approached, both $S_L(0)$ and ξ grow rapidly with decreasing temperature while $\bar{\eta}^2$ and ζ stay

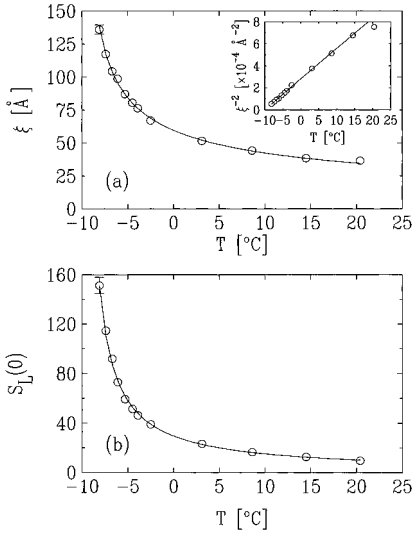

Figure 3. Temperature dependence of the fitting parameters for the Lorentzian component: (a) ξ; (b) $S_L(0)$. Lines are fits to the mean-field power laws in eq 2.

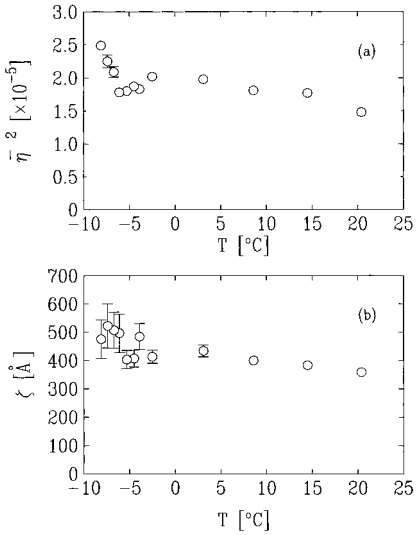

Figure 4. Temperature dependence of the fitting parameters for the "excess scattering": (a) $\bar{\eta}^2$; (b) ζ.

relatively constant. The insert in Figure 3a shows that mean-field power laws describe well the Lorentzian component of the structure factor at equilibrium. Fits of the correlation length ξ and $S_L(0)$ to the mean-field power laws in eq 2 are shown in Figure 3 as solid lines. From the fit of ξ we find the spinodal temperature $T_s = -9.9 \pm 0.2$ °C and exponent $\nu = 0.49 \pm 0.02$. The fit of $S_L(0)$ yields a spinodal temperature $T_s = -9.9 \pm 0.3$ °C and exponent $\gamma = 0.96 \pm 0.04$. The results from the two fits yield a consistent spinodal temperature and power law exponents which satisfy the $\gamma = 2\nu$ relation for the mean-field Ornstein−Zernicke correlation function. The spinodal temperature determined this way is in good agreement with that from cloud point measurements. The value of the prefactor ξ_0 obtained from the fit is 11.2 ± 0.7 Å.

4.2. Analysis of Early-Stage Spinodal Decomposition Kinetics. We have performed a series of temperature jumps from an anneal temperature of $T = 4.5$ °C above the coexistence curve to different final quench temperatures below the spinodal point. While we do not know the binodal temperature at this concentration, nucleation and growth of phase-separated regions in any metastable temperature range between

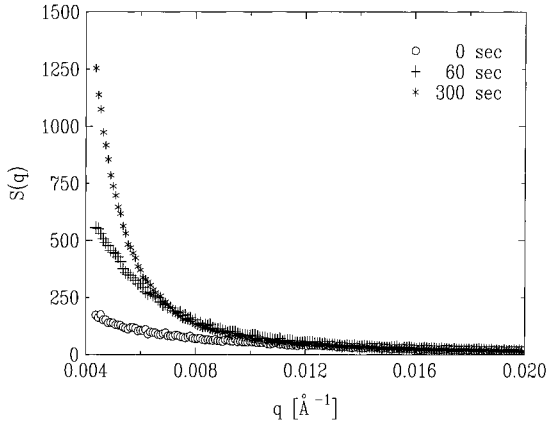

Figure 5. Structure factors at three different times after a quench. The anneal temperature is 4.5 °C, and the quench temperature is −14.0 °C.

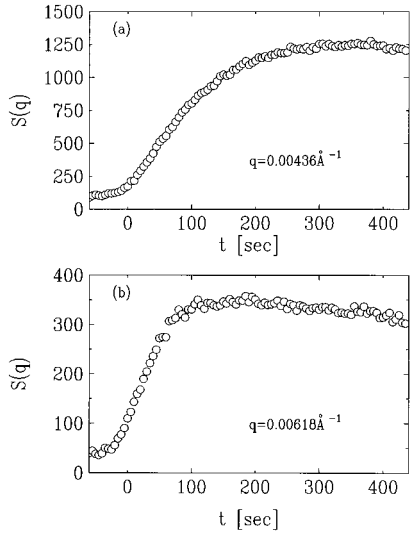

Figure 6. Time evolution of the structure factor at two different wavenumbers from the same quench as in Figure 5.

the measured spinodal and the unknown binodal points appear to be very sluggish. We never observed any changes in X-ray scattering patterns from these samples when they were held above the spinodal. Even anneals for 10 min at a temperature 2 deg above the spinodal gave no evidence of nucleation and growth occurring. We therefore conclude that no significant nucleation occurred while sample temperatures were passing through any metastable regime above the spinodal point. Quench temperatures range from −12.3 down to −29.3 °C. Following a quench, the temperature stabilized to within ±0.2 deg of the final temperature after approximately 40 s for shallow quenches and 120 s for deep quenches. For most of the quenches, there was relatively little growth of the structure factor before the temperature stabilized.

Figure 5 shows typical structure factor evolution at three different times after a quench, while Figure 6 plots the time evolution of the structure factor at fixed wavenumber q for two different wavenumbers. There is no peak in $S(q)$ in this wavenumber range during the measured time. These figures provide evidence that the spinodal decomposition has not yet reached the late-stage coarsening process. Any peak associated with coarsening domains would presumably be at lower q than was probed in this experiment. However, at wavenumbers well beyond the peak position in the coarsening regime, the structure factor would be expected to monotonically

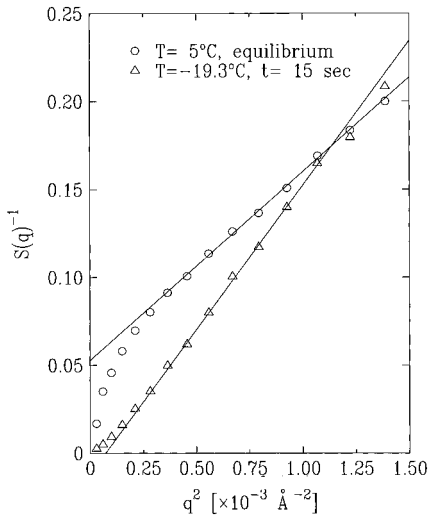

Figure 7. Zimm representation of structure factors indicating the intercept of the Lorentzian extrapolation changes sign before and after a quench.

decay with time and to exhibit a q^{-4} Porod power law dependence. Instead, the measured structure factor *grows* rapidly over most of the measured time interval at the lowest q values measured. At higher wavenumbers, the measured structure factor first grows, then reaches a peak in time, and finally decays. Moreover, no q^{-4} behavior is observed in the evolving structure factor at any time. These behaviors are difficult to explain if the sample is in the coarsening regime.

Since the sample appears to be in a relatively early stage of phase separation, we have used linear theory to analyze the time evolution of the structure factor. For simplicity, the time $t = 0$ is taken in the analysis to be when the temperature stabilizes. While some decomposition occurs before the temperature equilibrates, linear theory itself is invariant in form under a time translation. Therefore the linear theory analysis presented below is independent of the $t = 0$ choice. Since $S(q,t)$ is predicted to be a monotonic function of time by the linear theory, the fact that the structure factor decreases after reaching a maximum is a strong indication of nonlinearities in the kinetics at the time period and wavenumber range this is observed. The peaking of the structure factor in time occurs earlier for higher wavenumbers, suggesting that nonlinearities become important earlier at high wavenumbers than at low wavenumbers. A recent computer simulation study of the early-stage continuous ordering kinetics in a long range interaction Ising model also revealed that linear theory became a poor description of the kinetics earlier at higher wavenumbers.[10]

To approximately characterize the time of onset of strong nonlinearities, we extracted the time τ it takes for the structure factor to reach 90% of the maximum growth as a function of wavenumber. Since the kinetics was too fast to determine τ accurately at the highest wavenumbers examined, analysis was limited to $q < 0.01$ Å^{-1}. The time τ decreases with increasing wavenumber. Its wavenumber dependence is not a strict power law, but it approximately vaies as $\tau \sim q^{-2}$ at low wavenumbers (see Figure 8). The characteristic time τ for the shallow quenches is smaller than that for the deep quenches, suggesting nonlinearities become important at earlier times for shallow quenches than for deep quenches. This may be an effect of the exponentially activated mobility.

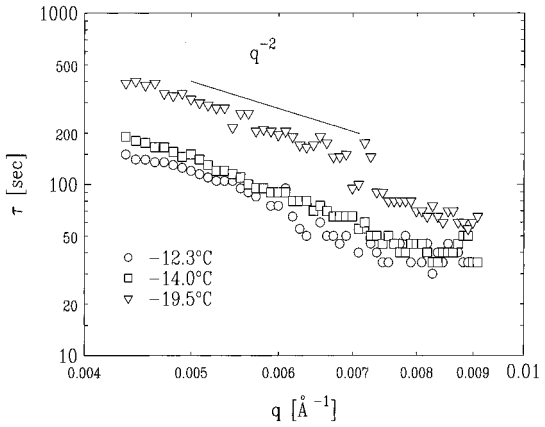

Figure 8. Time τ it takes for the structure factor to reach 90% of its maximum growth as a function of wavenumber.

Zimm plots of the observed structure factor before and after a quench are contrasted in Figure 7. The extrapolated intercept of the straight line fit for the intermediate wavenumber regime is positive for the equilibrium structure factor in the one-phase region. After a quench into the unstable two-phase region, the intercept initially changes sign from positive to negative. This is characteristic of the early-stage approach to $S(q,\infty)$ at high wavenumbers. In the late stages the short range fluctuations would equilibrate at the new quench temperature so that a positive intercept would again be observed. We also note that the magnitude of the scattering due to the phase separation process is 1 order of magnitude or more larger than the equilibrium scattering, so that the static "excess scattering" is not evident in the evolving structure factor.

To analyze the early-stage spinodal decomposition data according to linear theory, we have fit the time evolution of the structure factor at fixed wavenumber directly to the exponential form in eq 7. Both $R(q)$ and $S(q,\infty)$ are directly obtained as fitting parameters with appropriate error bars determined by the noise level of the data. The Onsager coefficient $\Lambda(q)$ is then calculated using eq 6. One has to be careful about the limitation of this method; i.e., the linear region must be determined before the fit is carried out. Fits of eq 7 to a set of data into times when nonlinearities become significant could result in incorrect $R(q)$ and $S(q,\infty)$ values. At the shallowest quench studied, to −12.3 °C, the kinetics were too fast and the scattering signal too low to determine the linear fit parameters accurately. It should be noted that these quenches are all relatively deep compared to those usually examined in light-scattering experiments of kinetics in polymer systems. Therefore the overall kinetic rate is dominated by the thermally activated mobility, which decreases with decreasing temperature, rather than the thermodynamic driving force which increases with increasing quench depth. Thus the kinetics is slower for deeper quenches, and only data from these are presented below.

Although the characteristic time τ mentioned above provides a model independent estimation of the time when nonlinearities become significant, a more accurate way of determining the linear region is desirable. We have used a "derivative analysis" which is directly based on the equation of motion in eq 5. At fixed wavenumber q, one plots $\partial S(q,t)/\partial t$ versus $S(q,t)$ with time t as an implicit variable. It can be seen from eq 5 that, if the structure factor changes according to linear theory, linear behavior is expected in this kind of plot. This

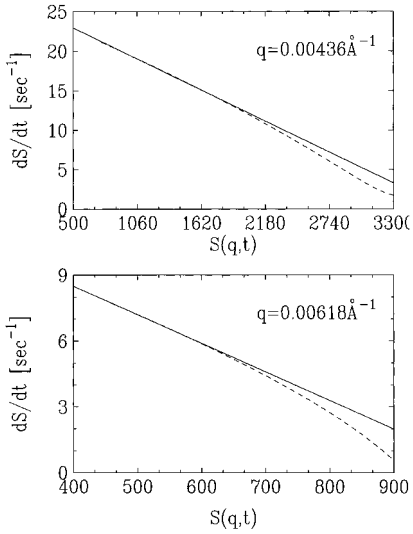

Figure 9. Typical dS/dt versus S plots at two different wavenumbers. The solution was annealed at 4.5 °C and quenched to −19.5 °C. The dashed line is smoothed data, and the solid line is the linear theory fit.

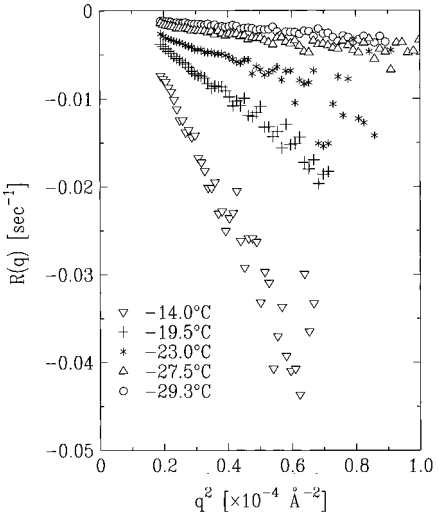

Figure 10. Wavenumber dependence of the relaxation rate $R(q)$. Quenches were from 4.5 °C to the final temperatures shown in the legend.

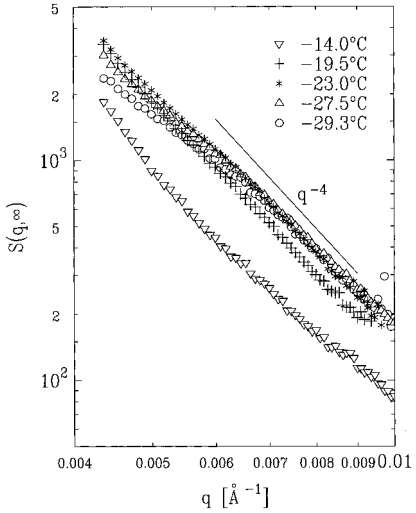

Figure 11. Wavenumber dependence of the virtual structure factor $S(q,\infty)$ for different quench temperatures, as indicated in the legend.

approach is very sensitive to the nonlinear terms omitted in eq 5 and can provide a test of the range of approximate validity of linear theory for spinodal decomposition kinetics. This information is used in the exponential fit analysis to determine the cutoff time for the fit. Since derivatives amplify any noise in the original data, a smoothing process was carried out prior to the "derivative analysis". Typical $\partial S(q,t)/\partial t$ versus $S(q,t)$ plots are shown in Figure 9; there is a linear region at early times so that the linear approximation can be used for the early-stage spinodal decomposition in our experiments. The growing importance of nonlinearities is evident from the deviation at later times from the initial linear behavior. The nonlinear behavior occurs first at higher wavenumbers.

The "derivative analysis" itself can also be used to determine values of the relaxation rate $R(q)$ and the Onsager coefficient $\Lambda(q)$ directly. If the initial linear part of the $\partial S(q,t)/\partial t$ versus $S(q,t)$ plot is fit to a straight line, the relaxation rate $R(q)$ is determined from the slope and $k_B T q^2 \Lambda(q)$ is determined from the intercept. This independently allows one to check the q dependence of the Onsager coefficient $\Lambda(q)$. The virtual structure factor $S(q,\infty)$ is then calculated using eq 6.

For comparison, we also analyzed our data using the "$^1/_3$ power plot" proposed by Sato and Han.[27] The results of the amplification factor $R(q)$ are found to be consistent from all three methods employed.

The relaxation rates $R(q)$ from the exponential fit are plotted as a function of q^2 for different quench temperatures in Figure 10. In the wavenumber range of this study, the $R(q)$ values are negative, which means we are above the critical wavenumber q_c where $R(q)$ changes sign. Throughout the wavenumber range, an approximate linear behavior in q^2 is observed, i.e., $R(q) \sim A - Bq^2$, where A and B are constants. This is consistent with the behavior of Binder's theory for $q > q_c$.

The virtual structure factors $S(q,\infty)$ obtained from the fits as a function of wavenumber for different quench temperatures are shown in Figure 11. The wavenumber dependence is approximately $S(q,\infty) \sim q^{-4}$. This is in contrast to the behavior in eq 8 predicted by Binder's theory using the random phase approximation. The Onsager coefficients $\Lambda(q)$ are calculated as a function of wavenumber for different quench temperatures from values of $R(q)$ and $S(q,\infty)$ using eq 6 and are shown in Figure 12. From this plot we find that $\Lambda(q) \sim q^{-4}$ throughout our wavenumber range. This is a much stronger wavenumber dependence than given by Binder's theory of eq 10.

5. Discussion and Conclusions

At intermediate wavenumbers ($q > 0.01$ Å$^{-1} \sim R_g^{-1}$), the evolution of the PS−DOP structure factor is broadly consistent with the predictions of existing early-stage kinetics theory using the random phase approximation. That is, $S(q,t)$ initially approaches a virtual structure factor which is a Lorentzian with a negative Zimm-plot intercept. In contrast the kinetics at low wavenumbers, where the "excess scattering" dominates the equilibrium structure factor, is not easily reconciled with existing early-stage kinetics theory. It is in this regime that the kinetics is sufficiently slow that we have been able to do the detailed analysis presented above. The time during which the linear theory treatment provides a reasonable description of the kinetics decreases with increasing wavenumber. Because of this effect, the appropriate time scale for fitting linear theory to the

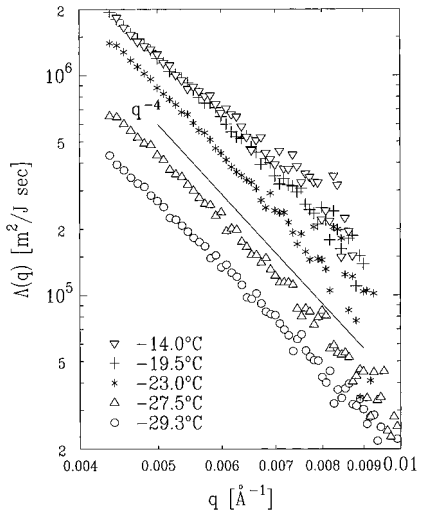

Figure 12. Wavenumber dependence of the Onsager coefficient $\Lambda(q)$ for different quench temperatures.

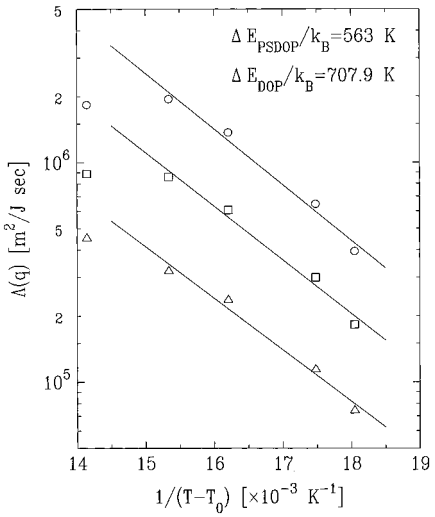

Figure 13. Temperature dependence of the Onsager coefficient at three different wavenumbers: (circles) 0.004 45 Å^{-1}; (squares) 0.005 54 Å^{-1}; (triangles) 0.007 09 Å^{-1}. Lines are fits to a Vogel−Fulcher functional from. The value $T_0 = 188.5$ K for pure DOP from ref 32 is used for the fits.

structure factor evolution should be determined at each wavenumber, as we have done with the "derivative analysis".

Both linear and nonlinear[28,29] approaches suggest that domains should form initially with a size comparable to a few correlation lengths following a quench into the spinodal region. This would cause a peak in the structure factor at q comparable to but less than ξ^{-1} at early times. Closely related to this issue is the change in sign of $R(q)$ and $S(q,\infty)$ expected from linear and nonlinear theories near ξ^{-1}. For the deep quenches examined in this study, extrapolation from above the spinodal would suggest that the correlation length should be relatively small, on the order of tens of angstroms, so that $\xi^{-1} \sim 0.02-0.03$ Å^{-1}. Hence, ξ^{-1} should be well within the experimental wavenumber range. However, none of the above features is in fact observed. This suggests either that the correlation lengths below the spinodal are very different than those above or that a larger length scale may be determining the kinetics. Our observations raise the possibility that inhomogeneities existing in the prequench state (which give rise to the "excess scattering") may be amplified during the early stages of spinodal decomposition and thus that the relevant length scale is the larger size ζ. It may be possible for future light scattering experiments to explore this issue.

There are a number of other suprises as well. First and foremost is the unexpected q^4 behavior of $S(q,\infty)$ and $\Lambda(q)$. It should be noted that the q^4 behavior in these quantities never occurs in $S(q,t)$ itself. It is also noteworthy that the experimental $S(q,\infty)$ values are quite large, 1 order of magnitude larger than the "excess scattering" or critical fluctuations observed even a few degrees above the spinodal line. Moreover, except for the shallow −14.0 °C quench, the virtual structure factors display little temperature dependence. The temperature dependence of $\Lambda(q)$ is generally consistent with expectations. That is, it is wavenumber-independent and (with the exception of the shallow −14.0 °C quench) can be fit to the Vogel−Fulcher form[30,31] with an activation energy comparable to that observed for the viscosity of pure DOP.[32]

A number of factors suggest that the analysis of the −14.0 °C quench may not be as accurate as that for the deeper quenches. The experimental $\Lambda(q)$ and $S(q,\infty)$ determined at −14.0 °C are too small relative to those measured at the deeper temperatures, as can readily be seen in Figures 11 and 12. Since the mobility is calculated from the fit $R(q)$ and $S(q,\infty)$ values via eq 6, it is not suprising that these two deviations occur together. It should be noted that the shallow quench data are the most difficult to analyze because the kinetics are faster than at lower temperatures and the scattering is smaller.

Clearly, there are important differences between the statics and kinetics observed in this semidilute solution and those predicted by the RPA approach. Whether these are entirely related to entanglements and screening in the solution, which are essentially neglected in the random phase approximation, is unknown. Previous theoretical work has assumed that $\Lambda(q)$ can be related to the relaxation behavior of single chains. In semidilute solutions where entanglements play a major role, this may be a poor approximation. It is perhaps noteworthy that the q^4 behavior of $S(q,\infty)$ and $\Lambda(q)$ cancels out to yield an amplification factor which does vary approximately linearly with q^2, as predicted by Binder's approach. Further theoretical advances are evidently required to understand the kinetics in semidilute solutions. From an experimental viewpoint, it would be quite interesting to examine kinetics in dilute solutions where entanglement effects are less important. Unfortunately, the associated decrease in viscosity would make the time scale of early-stage spinodal decomposition significantly shorter than that observed here. In addition, the magnitude of the scattering from a solution scales approximately as $c(1 - c)$, so that a decrease in concentration would lead to decreased scattering signal. We are currently evaluating the feasibility of such experiments.

Acknowledgment. We gratefully acknowledge the support of NSF-DMR and the NSF US-Czechoslovakia International Program. Part of this work was performed at the National Synchrotron Light Source, which is supported by the U.S. Department of Energy, Division of Materials Sciences and Division of Chemical Sciences (Contract No. DE-AC02-76CH00016). The MIT part of the IBM-MIT beamline X20 consortium is supported by the National Science Foundation. C.K. is supported by Grant Agency of the Academy of Sciences of the Czech

Republic No. 450416 and Grant Agency of the Czech Republic No. 203/94/0817.

References and Notes

(1) Gunton, J. D.; Miguel, M. S.; Sahni, P. S. *Phase Transitions and Critical Phenomena*; Academic Press: New York and London, 1983; Vol. 8.
(2) Hashimoto, T. *Phase Transitions* **1988**, *12*, 47.
(3) Cahn, J. W.; Hilliard, J. E. *J. Chem. Phys.* **1959**, *31*, 688.
(4) Cook, H. E. *Acta Metall.* **1970**, *18*, 297.
(5) de Gennes, P. G. *J. Chem. Phys.* **1980**, *72*, 4756.
(6) Pincus, P. *J. Chem. Phys.* **1981**, *75*, 1996.
(7) Binder, K. *J. Chem. Phys.* **1983**, *79*, 6387.
(8) Lal, J.; Bansil, R. *Macromolecules* **1991**, *24*, 290.
(9) Kuwahara, N.; Kubota, K. *Phys. Rev. A* **1992**, *45*, 7385.
(10) Gross, N.; Klein, W.; Ludwig, K. F. *Phys. Rev. Lett.* **1994**, *73*, 2639.
(11) Mainville, J.; Yang, Y. S.; Elder, K. R.; Sutton, M.; Ludwig, K. F.; Stephenson, G. B. To be published.
(12) deGennes, P. G. *Scaling Concepts in Polymer Physics*; Cornell University: Ithaca NY, and London, 1979.
(13) Stanley, H. E. *Introduction to Phase Transitions and Critical Phenomena*; Oxford University Press: Oxford, U.K., 1971.
(14) Benoit, H.; Picot, C. *Pure Appl. Chem.* **1966**, *12*, 1271.
(15) Dautzenberg, H. *J. Polym. Sci., Part C* **1972**, *39*, 123.
(16) Koberstein, J. T.; Picot, C.; Benoit, H. *Polymer* **1985**, *26*, 673.
(17) Gan, J. Y. S.; Francois, J.; Guenet, L.-M. *Macromolecules* **1986**, *19*, 173.
(18) Xie, Y.; Ludwig, K. F.; Gallagher, P. D.; Bansil, R.; Cao, X. To be published.
(19) Debye, P.; Bueche, A. M. *J. Appl. Phys.* **1949**, *20*, 518.
(20) Benoit, H.; Benmouna, M. *Polymer* **1984**, *25*, 1059.
(21) Kuwahara, N.; Kubota, K.; Sakazume, M.; Eda, H.; Takiwaki, K. *Phys. Rev. A* **1992**, *45*, R8324.
(22) Schwahn, D.; Janssen, S.; Springer, T. *J. Chem. Phys.* **1992**, *97*, 8775.
(23) Jinnai, H.; Hasegawa, H.; Hashimoto, T.; Han, C. *J. Chem. Phys.* **1993**, *99*, 8154.
(24) Stephenson, G. B.; Ludwig, K. F.; Jordan-Sweet, J. L.; Brauer, S.; Mainville, J.; Yang, Y. S.; Sutton, M. *Rev. Sci. Instrum.* **1989**, *60*, 1537.
(25) Berry, G. C. *J. Chem. Phys.* **1966**, *44*, 4550.
(26) desCloizeaux, J.; Jannink, G. *Les Polymeres en Solution: leur Modelization et leur Structure*; Les editions de physique: Paris, 1987.
(27) Sato, T.; Han, C. C. *J. Chem. Phys.* **1988**, *88*, 2057.
(28) Langer, J. S.; Bar-on, M.; Miller, H. D. *Phys. Rev. A* **1975**, *11*, 1417.
(29) Grant, M.; Miguel, M. S.; Vials, J.; Gunton, J. D. **1985**, *31*, 3027.
(30) Vogel, H. *Phys. Z.* **1921**, *22*, 645.
(31) Fulcher, G. S. *J. Am. Ceram. Soc.* **1925**, *6*, 339.
(32) Stepanek, P. Ph.D. Thesis, IMC Prague, 1981.

MA950153K